High Rate Pulse Processing Algorithms for Microcalorimeters

Hui Tan[a], Dimitry Breus[a], Wolfgang Hennig[a], Konstantin Sabourov[a], Jeffrey W. Collins[a], William K. Warburton[a], W. Bertrand Doriese[b], Joel N. Ullom[b], Minesh K. Bacrania[c], Andrew S. Hoover[c], Michael W. Rabin[c]

[a]*XIA LLC, 31057 Genstar Rd., Hayward, CA 94544, USA*
[b]*National Institute of Standards and Technology, 325 Broadway, Boulder, CO 80305, USA*
[c]*Los Alamos National Laboratory, Los Alamos, NM 87545, USA*

Abstract. It has been demonstrated that microcalorimeter spectrometers based on superconducting transition-edge-sensors can readily achieve sub-100 eV energy resolution near 100 keV. However, the active volume of a single microcalorimeter has to be small in order to maintain good energy resolution, and pulse decay times are normally on the order of milliseconds due to slow thermal relaxation. Therefore, spectrometers are typically built with an array of microcalorimeters to increase detection efficiency and count rate. For large arrays, however, as much pulse processing as possible must be performed at the front end of readout electronics to avoid transferring large amounts of waveform data to a host computer for post-processing. In this paper, we present digital filtering algorithms for processing microcalorimeter pulses in real time at high count rates. The goal for these algorithms, which are being implemented in readout electronics that we are also currently developing, is to achieve sufficiently good energy resolution for most applications while being: a) simple enough to be implemented in the readout electronics; and, b) capable of processing overlapping pulses, and thus achieving much higher output count rates than those achieved by existing algorithms. Details of our algorithms are presented, and their performance is compared to that of the "optimal filter" that is currently the predominantly used pulse processing algorithm in the cryogenic-detector community.

Keywords: microcalorimeter, optimal filter, algorithms and implementation.
PACS: 07.20.Mc, 87.55.kd, 07.05.Kf, 84.30.Sk.

INTRODUCTION

Superconducting transition edge sensor (TES) based microcalorimeters can be used as very precise detectors for electromagnetic radiation from the near-infrared to gamma rays. Their energy resolution is fundamentally limited only by the ratio of the measured temperature rises to the value of thermodynamic temperature fluctuations. For example, a cryogenic gamma-ray detector based on TES can achieve a resolution well below 100 eV near 100 keV [1]. However, individual microcalorimeters are relatively small (to maintain good energy resolution) and slow (due to the sensor's thermal relaxation). Further, existing microcalorimeter pulse processing algorithms, e.g. optimal filtering [2], typically reject overlapping (piled-up) pulses when computing pulse heights, and normally run on an offline PC. Consequently, detection efficiency is low and output count rates are limited. This is typically solved by building systems with an array of microcalorimeters. Large arrays, however, require that much pulse processing as possible be performed at the front end of readout electronics to avoid transferring large amounts of waveform data to a host computer for processing.

The main motivation of this paper is to develop pulse processing algorithms that can: 1) be implemented in the readout electronics to perform real time digital signal processing; 2) achieve energy resolution comparable to that is achieved by optimal filtering; and, 3) be able to process overlapping microcalorimeter pulses so that output count rate can be significantly improved when compared to the rate capability of optimal filtering.

In order to be able to process overlapping pulses, we need to know each pulse's exact shape so that we can correct the height of the current pulse if it sits on the tail part of a previous pulse. This is illustrated in Figure 1. A running sum filter, RS, which is the

summation of L digitized trace data samples, is continuously updated upon the arrival of each new digitized trace data point. When a pulse is detected through a separate trigger filter, the algorithm looks for the time when the running sum RS reaches its maximum. At that time, RS is stored, and B, the contribution to the running sum from the preceding pulse, is computed. The pulse height is then represented by the value of filter response (RS - B) / L, or J / L, where J is the net area under the pulse when RS reaches its maximum as shown in Figure 1. It is relatively straightforward to estimate B if the preceding part of a pulse is flat, e.g. the first pulse shown in Figure 1. However, to estimate B for a pulse sitting on the tail part of the previous pulse, e.g. the second pulse in Figure 1, the shape of the preceding pulse's tail needs to be known in detail.

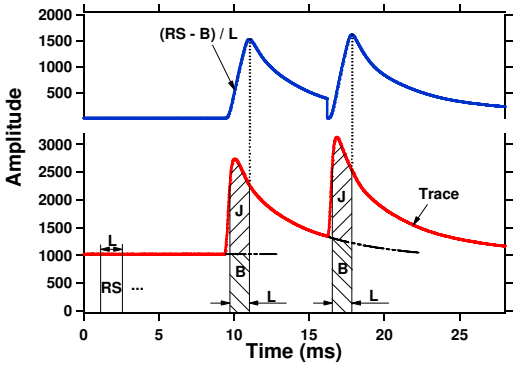

FIGURE 1. Illustration of calculating pulse height for microcalorimeter pulses.

Our high rate pulse processing algorithms focus on how to accurately estimate B for overlapping pulses. We will first derive the formulas for the pulse processing algorithms, next apply these algorithms to previously acquired microcalorimeter pulse data files, and then finally discuss the results.

FILTER ALGORITHMS

Typical TES based microcalorimeter pulses can be characterized by one rising time constant and one or more decay time constants. The number of exponential decay time constants depends on the structure and material composition of the detectors. For instance, an X-ray detector normally has one heat capacity and one thermal conductance, resulting in a single decay time constant. On the other hand, compound gamma-ray detectors with an absorber glued to the TES typically have two heat capacities and thermal conductances, and thus two or more decay time constants. Therefore, we present below filter algorithms for processing microcalorimeter pulses with single, double, or triple decay time constants. Detectors producing pulses with more than three decay time constants are rare. Assume the three decay time constants can be represented as τ_i, i = 1, 2, 3, and ΔT is the trace sampling interval (16 μs in the analysis below), in the following we define

$$\beta_i = e^{-\frac{\Delta T}{\tau_i}} \quad (1)$$

$$\delta_{i,L} = \beta_i^L - 1 \quad (2)$$

$$\chi_{i,L} = \frac{\beta_i^L - 1}{\beta_i - 1} \quad (3)$$

Pulses with single decay time constant

Figure 2 illustrates one pulse overlapping a preceding pulse with a single decay time constant τ_1. Four consecutive running sums, RS_1 to RS_4 with the same length L, are accumulated. DC is the amplitude of the trace when no pulse is presented (baseline), and A_1 is the trace amplitude minus DC at the beginning of RS_1.

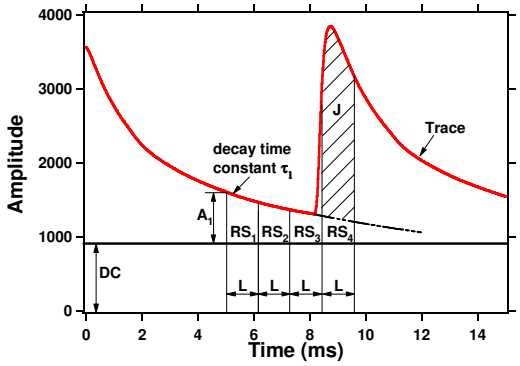

FIGURE 2. Illustration of calculating pulse height for microcalorimeter pulses with single decay time constant.

Running sums RS_1, RS_2 and RS_4 can then be expressed as follows.

$$RS_i = DC + A_1 \beta_1^{(i-1)L} \chi_{1,L}, i = 1,2 \quad (4)$$

$$RS_4 = DC + A_1 \beta_1^{3L} \chi_{1,L} + J \quad (5)$$

DC and J can be easily solved by substituting the unknown A_1 with the known running sums and decay time constant. Note that even though running sum RS_3 is not being used for calculating either DC or J, its existence is necessary to prevent RS_2 from cutting into the rising edge of the second pulse.

$$DC = \frac{1}{\delta_{1,L}} \left(\beta_1^L RS_1 - RS_2 \right) \quad (6)$$

$$J = \left(RS_4 - DC \right) - \beta_1^{3L} \left(RS_1 - DC \right) \quad (7)$$

Pulses with double decay time constants

Figure 3 shows how to calculate pulse height for pulses with double decay time constants τ_1 and τ_2. Five consecutive running sums, RS_1 to RS_5, are continuously updated as new trace sample data arrives. A_1 and A_2 are the trace amplitude minus DC at the

beginning of RS_1 for exponential decay components with time constants τ_1 and τ_2, respectively.

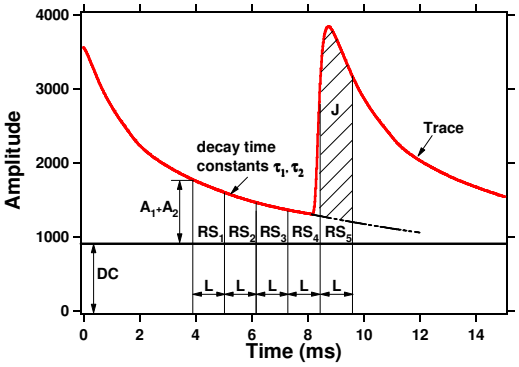

FIGURE 3. Illustration of calculating pulse height for microcalorimeter pulses with double decay time constants.

Running sums RS_1, RS_2, RS_3 and RS_5 can be expressed as follows. DC and J were then solved by using Mathematica®.

$$RS_i = DC + A_1\beta_1^{(i-1)L}\chi_{1,L} + A_2\beta_2^{(i-1)L}\chi_{2,L}, i = 1,2,3 \quad (8)$$

$$RS_5 = DC + A_1\beta_1^{4L}\chi_{1,L} + A_2\beta_2^{4L}\chi_{2,L} + J \quad (9)$$

$$DC = \frac{1}{\delta_{1,L}\delta_{2,L}}\left(\beta_1^{L}\beta_2^{L}RS_1 - \left(\beta_1^{L} + \beta_2^{L}\right)RS_2 + RS_3\right) \quad (10)$$

$$J = \beta_1^{L}\beta_2^{L}\left(\beta_1^{2L} + \beta_1^{L}\beta_2^{L} + \beta_2^{2L}\right)(RS_1 - DC) - \left(\beta_1^{L} + \beta_2^{L}\right)\left(\beta_1^{2L} + \beta_2^{2L}\right)(RS_2 - DC) + (RS_5 - DC) \quad (11)$$

Pulses with triple decay time constants

To solve for J for pulses with triple decay time constants, six running sums, RS_1 to RS_6, are needed. As shown in Figure 4, A_1, A_2 and A_3 are the trace amplitude minus DC at the beginning of RS_1 for exponential decay components with time constants τ_1, τ_2 and τ_3, respectively.

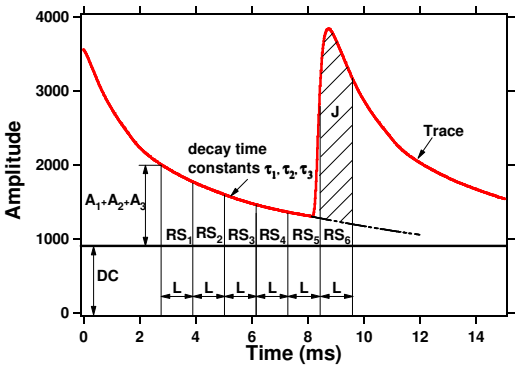

FIGURE 4. Illustration of calculating pulse height for microcalorimeter pulses with triple decay time constants.

Running sums RS_1, RS_2, RS_3, RS_4 and RS_6 are first expressed as follows. DC and J were then again solved by using Mathematica®.

$$RS_i = DC + A_1\beta_1^{(i-1)L}\chi_{1,L} + A_2\beta_2^{(i-1)L}\chi_{2,L} + A_3\beta_3^{(i-1)L}\chi_{3,L}, i = 1-4 \quad (12)$$

$$RS_6 = DC + A_1\beta_1^{5L}\chi_{1,L} + A_2\beta_2^{5L}\chi_{2,L} + A_3\beta_3^{5L}\chi_{3,L} + J \quad (13)$$

$$DC = \frac{1}{\delta_{1,L}\delta_{2,L}\delta_{3,L}}\left(-\beta_1^{L}\beta_2^{L}\beta_3^{L}RS_1 + \left(\beta_1^{L}\beta_2^{L} + \beta_1^{L}\beta_3^{L} + \beta_2^{L}\beta_3^{L}\right)RS_2 - \left(\beta_1^{L} + \beta_2^{L} + \beta_3^{L}\right)RS_3 + RS_4\right) \quad (14)$$

$$J = -\beta_1^{L}\beta_2^{L}\beta_3^{L}\left(\beta_1^{2L} + \beta_2^{2L} + \beta_2^{L}\beta_3^{L} + \beta_3^{2L} + \beta_1^{L}\left(\beta_2^{L} + \beta_3^{L}\right)\right)(RS_1 - DC) + \left(\beta_1^{3L}\left(\beta_2^{L} + \beta_3^{L}\right) + \beta_1^{2L}\left(\beta_2^{L} + \beta_3^{L}\right)^2 + \beta_2^{L}\beta_3^{L}\left(\beta_2^{2L} + \beta_2^{L}\beta_3^{L} + \beta_3^{2L}\right) + \beta_1^{L}\left(\beta_2^{L} + \beta_3^{L}\right)\left(\beta_2^{2L} + \beta_2^{L}\beta_3^{L} + \beta_3^{2L}\right)\right)(RS_2 - DC) - \left(\beta_1^{3L} + \beta_1^{2L}\left(\beta_2^{L} + \beta_3^{L}\right) + \left(\beta_2^{L} + \beta_3^{L}\right)\left(\beta_2^{2L} + \beta_3^{2L}\right) + \beta_1^{L}\left(\beta_2^{2L} + \beta_2^{L}\beta_3^{L} + \beta_3^{2L}\right)\right)(RS_3 - DC) + (RS_6 - DC) \quad (15)$$

For all the three cases of decay time constants discussed above, the filters can be slightly modified by only making the length of the last running sum, which includes pulse's net area J, be different from the length of all other running sums. Running sums can then be expressed similarly, and DC and J can be solved accordingly.

IMPLEMENTATION OF FILTER ALGORITHMS IN HARDWARE

Our filter algorithms will be implemented in field programmable gate arrays (FPGAs) to calculate pulse heights and accumulate energy histograms in real time. Modern FPGAs have dedicated multipliers and can be configured to perform the numerical computations as described above even for many channels in parallel, e.g. multiplexed data from multiple microcalorimeter pixels. With known pulse shapes (decay time constants) and user specified running sum lengths, a set of filter coefficients can be computed by the host control software and downloaded to the FPGAs before the start of the data acquisition. In real time the FPGAs then only need to multiply the coefficients with individual running sums, add the multiplication results together to get the pulse height, and finally histogram the pulse height into energy histograms.

RESULTS AND DISCUSSIONS

The filter algorithms were applied offline to a set of microcalorimeter data files taken at LANL in October 2008. Each file contains 2 hours of streamed data from a ^{153}Gd source and a 14-pixel array manufactured by NIST. For illustration purposes, only results from the best performing pixel (channel 19 as indicated by the file names) are shown here. Two data files from this pixel, each at different input count rates (ICRs), ~3 cps and ~11 cps, respectively, were used in the analysis. Best described by three decay time constants, pulses in these data files were individually fitted to determine their decay times, due to their dependence on pulse height (at 97 keV, τ_1, τ_2 and τ_3 are

~1 ms, 4.4 ms, and 27.6 ms, respectively). Thus the XIA filter with six running sums was used, and the length of the last running length was fixed at its optimal value of 1.2 ms. Figure 5 shows the resulting ^{153}Gd pulse height spectrum at ICR ~3 cps. The inset illustrates that the closely neighboring peaks at 70 – 80 keV can be resolved very well.

Figure 6 displays the measurement of the linearity of the algorithms by plotting the measured energies versus known energies of ^{153}Gd after calibrating the pulse height spectrum (Figure 5) using the 97.43 keV peak. The optimal filter used two energies, 97.43 keV and 103.18 keV, to calibrate its spectrum. The XIA filter demonstrated excellent linearity at all energies with the largest deviation of 0.75% at 68.94 keV. The optimal filter showed slight deviations from theoretical energies at lower energies with the largest deviation of 5.28% at 68.94 keV.

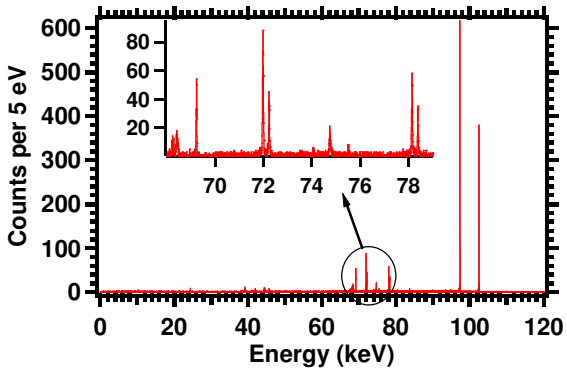

FIGURE 5. Pulse height spectrum from a ^{153}Gd source and an array of 14-pixel microcalorimeters manufactured by NIST and measured at LANL.

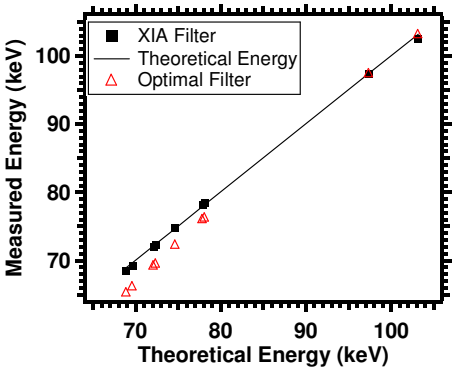

FIGURE 6. Linearity between theoretical and measured energies.

Length of running sums was varied to measure its effect on the energy resolution as shown in Figure 7. The bottom axis is the total length of the six running sums (RS_1 to RS_5 have equal lengths and RS_6's length was fixed at 1.2 ms), which is also the pileup rejection length. The left axes are the energy resolution (FWHM) at 97.43 keV, the pileup loss percentage, and the MTOCR (maximal theoretical output count rate), respectively. The best energy resolution was achieved at a filter length of 33.2 ms for both input count rates, and the corresponding MTOCR is ~11 cps. A higher MTOCR can be achieved with shorter total length when sub-optimum energy resolution is acceptable.

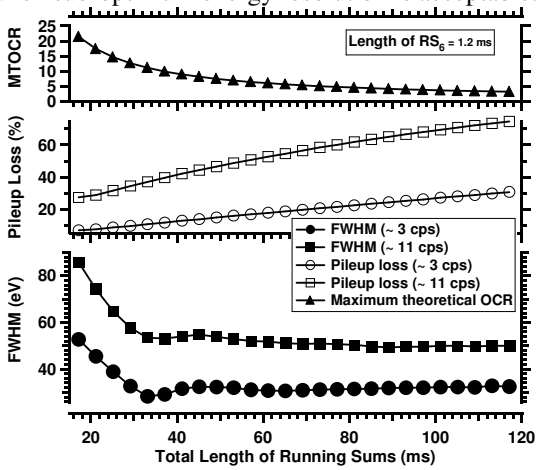

FIGURE 7. Energy resolution, pileup loss and maximum theoretical OCR as a function of the total length of running sums.

TABLE 1. Performance comparison of optimal filter to XIA filter.

Best Energy Resolution at 97 keV, Corresponding Pileup Loss	Optimal Filter	XIA Filter
FWHM (eV) (~ 3 cps)	29.7	28.2
Pile-up Loss (~ 3 cps)	41.3%	10.7%
FWHM (eV) (~ 11 cps)	55.6	53.0
Pile-up Loss (~ 11 cps)	71.5%	39.6%

Table 1 summarizes the performance comparison between the optimal filter and the XIA filter. At ~3 cps, XIA filter yielded the best energy resolution of 28.2 eV FWHM and a corresponding pileup loss of 10.7% when the total running sums length was 33.2 ms. At ~11 cps, the energy resolution achieved by the XIA filter is still slightly better than that of the optimal filter, and its pileup loss is almost a factor of two smaller than the loss by the optimal filter.

ACKNOWLEDGMENTS

This work was sponsored by the U.S. Department of Energy under Grant DE-FG02-07ER84760.

REFERENCES

1. M. K. Bacrania, A. S. Hoover, and 14 co-authors, *IEEE Trans. Nucl. Sci.* **56**, 2299-2302 (2009).
2. A. E. Szymkowiak, R. L. Kelley, S. H. Moseley and C. K. Stahle, *J. Low Temp. Phys.* **93**, 281-285 (1993).